The Astrophysical Journal, 599:164–172, 2003 December 10

DOES THE IRON Kα LINE OF ACTIVE GALACTIC NUCLEI ARISE FROM THE CERENKOV LINE–LIKE RADIATION?

J. H. You,[1] D. B. Liu,[1] W. P. Chen,[2] L. Chen,[1] and S. N. Zhang[3,4,5]

Received 2003 January 27; accepted 2003 August 19

ABSTRACT

When thermal relativistic electrons with isotropic distribution of velocities move in a gas region or impinge upon the surface of a cloud that consists of a dense gas or doped dusts, the Cerenkov effect produces peculiar atomic or ionic emission lines, which is known as the Cerenkov line–like radiation. This newly recognized emission mechanism may find wide applications in high-energy astrophysics. In this paper we tentatively adopt this new line emission mechanism to discuss the origin of the iron Kα feature of active galactic nuclei (AGNs). The motivation of this research is to attempt a solution to a problem encountered by the "disk fluorescence line" model, i.e., the lack of temporal response of the observed iron Kα line flux to the changes of the X-ray continuum flux. If the Cerenkov line emission is indeed responsible significantly for the iron Kα feature, the conventional scenario around the central supermassive black holes of AGNs would need to be modified to accommodate more energetic, more violent, and much denser environments than previously thought.

Subject headings: galaxies: active — radiation mechanisms: nonthermal — X-rays: galaxies

1. INTRODUCTION

Observations in the last decade show that many active galactic nuclei (AGNs), e.g., the Seyfert 1 galaxies, display in their spectra an emission feature peaked around ~6.4–6.5 keV, commonly attributed to the Kα line emission of iron ions in low- or intermediate-ionization states. The observed Kα line is very broad, and the line profile is asymmetric, being steep on the blue and flattening on the red wavelength wing, extending to 4–5 keV, as shown in Figure 1 (Tanaka et al. 1995; Nandra et al. 1997a, 1997b; Fabian et al. 2002; Wang, Wang, & Zhou 2001). The iron Kα is regarded as one of the best probes to explore the physical mystery in regions proximate to the central supermassive black holes of AGNs. Its observation and interpretation thus have drawn great attention lately in black hole and AGN study.

So far the prevailing model is based on the "photoelectric absorption fluorescence line emission" mechanism (e.g., Guilbert & Rees 1988; Fabian et al. 1989; Reynolds 2001), which has gained wide popularity because it successfully produces a line profile consistent with observations. Furthermore, the underlying emission mechanism, that is, photoelectric absorption followed by fluorescence line emission, has been so far taken for granted as the only way to produce the X-ray atomic or ionic emission line by heavy ions in low- or intermediate-ionization states for which the K shell of the ion is fully filled. Take an iron ion as an example: because the K shell is fully closed, the transition $n = 2 \rightarrow 1$ (Kα) cannot occur unless certain external X-ray illumination causes photoelectric absorption to first make a "vacancy" in the K shell.

Despite the success of the photoelectric absorption fluorescence line mechanism, we suggest an alternative mechanism—the Cerenkov line–like radiation—to explore the origin of iron Kα in AGNs. The motivation of this research is to attempt a solution of a problem encountered by the "disk fluorescence line" model, i.e., the temporal response of the iron Kα line flux to the changes of the X-ray continuum flux, predicted by a simple photoelectric absorption fluorescence line emission model. So far no clear response of line flux to the incident X-rays has been observed (e.g., Lee et al. 1999, 2000; Chiang et al. 2000; Wang et al. 1999, 2001; Weaver, Gelbord, & Yaqoob 2001). It has been suggested that a flux-correlated change of ionization states of the iron ions would be responsible for the lack of correlation between the fluxes of iron Kα line and the continuum (e.g., Reynolds 2001). This may well be true and deserves to be given a further quantitative analysis to confirm this viewpoint. There is another model that attempts to explain the lack of temporal response. Vaughan, Fabian, & Nandra (2003) and Miniutti et al. (2003) suggest a model in which the X-ray source is close to the spin axis of the black hole and the long-timescale changes (>10 ks) are due to changing height of this source. The light-bending effect can then produce an almost constant line intensity together with a changing observed continuum flux. In this paper we try to give another explanation for this problem by using the newly recognized Cerenkov line emission mechanism.

In § 2 of this paper we first outline the physics of the new line emission mechanism to help people who are unfamiliar with this mechanism. Relevant basic formulae are presented in the Appendix. Besides, we discuss the conditions under which the new emission mechanism becomes predominant over the photoionization fluorescence process and should be taken into consideration to explore the origin of the iron Kα line in AGNs. In § 3 we give some model considerations and model calculations by use of the new mechanism to match the observed luminosities of the iron Kα line and, in

[1] Institute for Space and Astrophysics, Department of Physics, Shanghai Jiao-Tong University, Shanghai 200030, China; jhyou@online.sh.cn.
[2] Institute of Astronomy and Department of Physics, National Central University, Chung-Li 32054, Taiwan, China.
[3] Center for Astrophysics, Department of Physics, Tsinghua University, Beijing 100084, China.
[4] Department of Physics, University of Alabama in Huntsville, Huntsville, AL 35899.
[5] National Space Science and Technology Center, 320 Sparkman Drive, SD50, Huntsville, AL 35805.

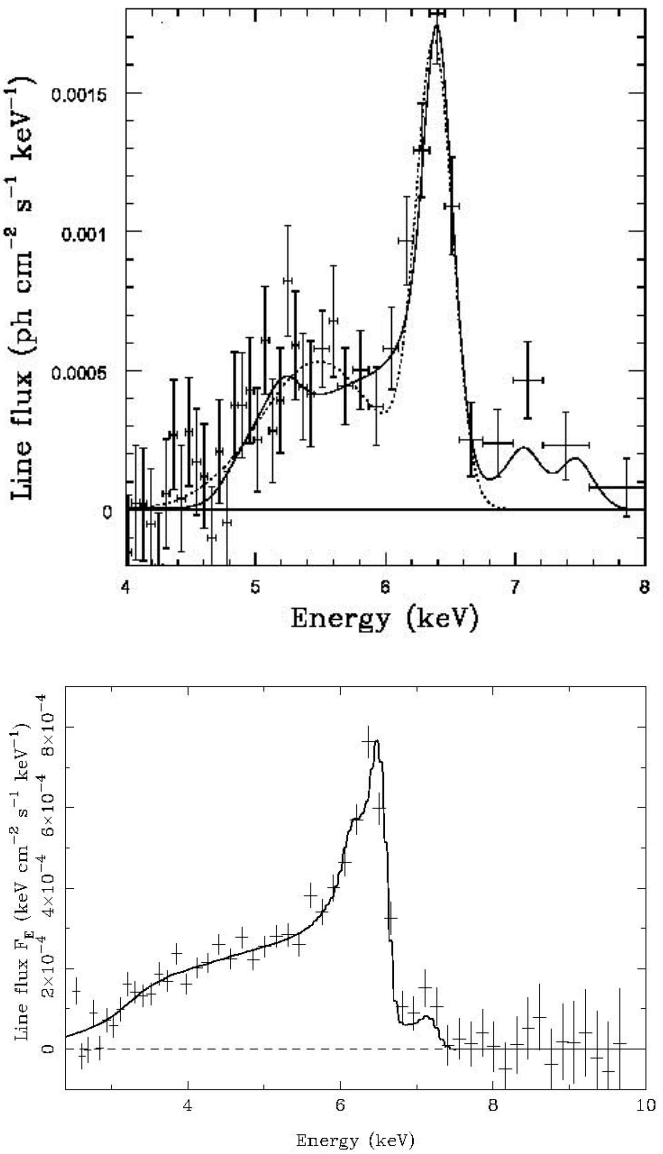

FIG. 1.—Observed iron Kα line of Seyfert 1 galaxy NGC 4151 (*top*; taken from Wang et al. 2001) and MCG −6-30-15 (*bottom*; taken from Fabian et al. 2002). The small linelike hump at ~7–8 keV (in rest frame) is due to the iron Kβ line emission.

turn, to see whether the estimated environmental parameters are reasonable and acceptable in regions proximate to the central supermassive black hole of AGNs. In § 4 we provide conclusions and discussions.

2. CERENKOV LINE–LIKE RADIATION AS THE RESPONSIBLE MECHANISM: OUTLINE OF PHYSICS OF THE NEW MECHANISM

In this paper we propose that the Cerenkov line–like radiation (You & Cheng 1980; You et al. 1986, 2000) could be responsible for the iron emission feature in AGNs. We shall show that this emission mechanism may become predominant over the fluorescence process under certain conditions around AGNs. Furthermore, the possible difficulty encountered by the fluorescence mechanism as mentioned above, namely, the lack of correlation between the line and the continuum fluxes, can be alleviated because the radiation energy of the Cerenkov line is provided by relativistic electrons rather than by the X-ray continuum as in the fluorescence process.

The Cerenkov line–like mechanism has been confirmed by elegant laboratory experiments in O_2, Br_2, and Na vapor using a ^{90}Sr β-ray source with the fast coincidence technique (Xu, Yang, & Xi 1981, 1988, 1989). Detailed discussions on the basic physics and improved formulae have been further presented recently (You et al. 2000). Here we outline the physics and essential results of the theory to help the people who are unfamiliar with this new mechanism. The relevant basic formulae are presented in the Appendix for people who are interested in the theory of Cerenkov line–like radiation.

When the thermal relativistic electrons with isotropic distribution of velocities move in a gas region or impinge upon the surface of a dense cloud with arbitrary shape (e.g., with filamentary-like or sheetlike structure), Cerenkov radiation is produced within a narrow wavelength range $\Delta\lambda$, very close to the intrinsic atomic or molecular wavelength λ_{lu} (u and l denoting, respectively, the corresponding upper and lower energy levels) because only in this narrow band is the refractive index of gas significantly larger than one, $n > 1$, which makes it possible to satisfy the Cerenkov radiation condition $n \geq c/v \equiv 1/\beta$. The emission feature therefore appears more like an atomic or molecular line than a continuum, thus the name "Cerenkov line–like radiation" or simply "Cerenkov emission line."

For a gaseous medium, the dispersion curve $n \sim \lambda$ and the resonant line absorption curve $\kappa \sim \lambda$ can be calculated exactly by using the formula of the refractive index for gas, $(\tilde{n}^2 - 1)/(\tilde{n}^2 + 2) = (4\pi/3)N\alpha$, where $\tilde{n} = n - i\kappa$ is the complex refractive index, with the real part n being the refractive index of gas and the imaginary part κ being the extinction coefficient that relates with the line absorption coefficient by a simple formula $k_{lu} = (4\pi\nu/c)\kappa_\nu$ (You et al. 2000, or eq. [A3] in the Appendix); N is the number density of the atomic/molecular species; and α is the polarizability per atom or ion, given by quantum theory (You et al. 2000). For a very dense gas, n is large. For $\lambda \approx \lambda_{lu}$, the value of α, and hence the value of n, becomes very large (see the schematic dispersion curve $n^2 \sim \lambda$ in Fig. 2). We emphasize that $n > 1$ at $\lambda \gtrsim \lambda_{lu}$ is valid even when the lower energy level l is fully closed, as long as the upper level u is not completely filled (see eq. [A1] in the Appendix). This is substantially different from the fluorescence emission, which always requires one to preempt a vacancy in the lower level. It is this unique property that makes it easier to produce the Kα line of iron ions in intermediate-ionization states by the Cerenkov mechanism, under certain circumstances, than by the fluorescence process.

In Figure 2 we see that a strong resonant absorption occurs at $\lambda = \lambda_{lu}$ where the Cerenkov radiation vanishes. The Cerenkov mechanism only operates in the narrow shaded region $\lambda > \lambda_{lu}$, where the absorption approaches zero, $\kappa_\lambda \to 0$. The combination of absorption and emission causes the final emission feature to be slightly redshifted, which we call "Cerenkov line redshift" in order to distinguish it from other types of redshift mechanisms (Doppler, gravitational, Compton, etc.). As we shall show below, the Cerenkov line redshift is favorable to increase the emergent flux of the Cerenkov emission line from the surface of a dense cloud.

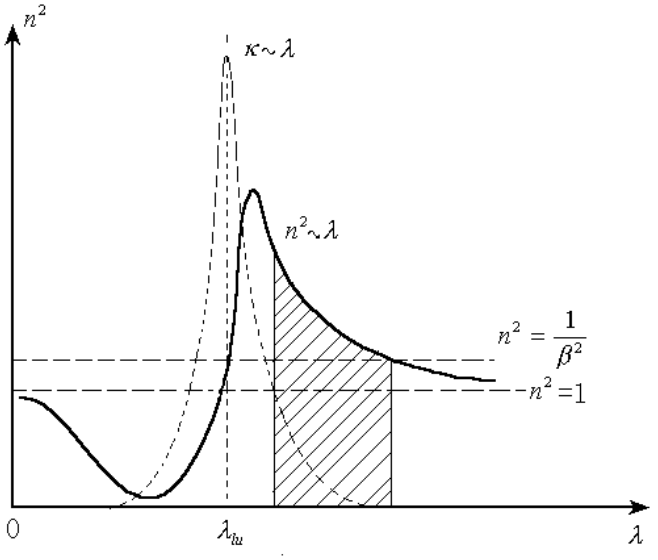

FIG. 2.—Schematic sketch of the dispersion curve of gas $n^2 \sim \lambda$ and the curve $\kappa \sim \lambda$, where κ is the extinction coefficient of gas, which relates with the line absorption coefficient by a simple formula $k_\lambda = (4\pi/\lambda)\kappa_\lambda$. The Cerenkov radiation survives in the shaded narrow region where the Cerenkov radiation condition $n \geq 1/\beta$ is satisfied and where the extinction is small. The shaded region is narrow, making the emerging radiation appear more like a line emission than a continuum.

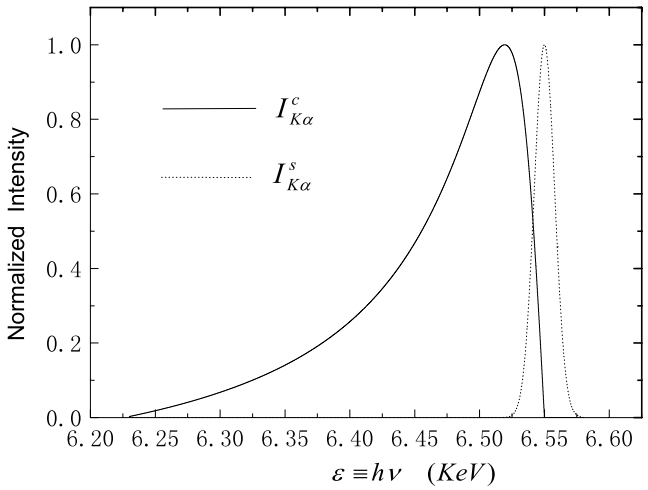

FIG. 3.—Calculated profile of the Cerenkov line $I^c_{K\alpha} \sim \varepsilon$ of iron ion Fe^{+21} in the optically thick case, assuming $N_{Fe} = 10^{17}$ cm^{-3} and $\gamma_c = 2 \times 10^5$, where $\varepsilon \equiv h\nu$ is the energy of the line photon. The Cerenkov line profile is broad, asymmetric, and redshifted. The profile of a normal line by spontaneous transition $I^s_{K\alpha} \sim \varepsilon$ is also plotted for comparison.

In summary, the Cerenkov line–like emission has the following characteristics: (1) It is concentrated in a small wavelength range, so it appears more like a line than continuum. The denser the gas, the broader the emission "line" feature. (2) If the dense gas is optically thick for the Cerenkov line emission, the emergent line profile becomes asymmetric, being steep on the high-energy side and flattened on the low-energy side. (3) The peak of the emission feature is not exactly at $\lambda = \lambda_{lu}$ but slightly redshifted as a result of the line absorption shown in Figure 2. In the optically thick case, the typical value of Cerenkov line redshift would be as high as $z \sim 10^{-3}$ (You et al. 2000), which in terms of Doppler effect would correspond to an apparent velocity of several hundred kilometers per second. (4) The radiation would be polarized if the relativistic electrons have an anisotropic velocity distribution.

Figure 3 shows the calculated profile of the Cerenkov Kα line of Fe^{+21} in the optically thick case. For comparison a normal line by a spontaneous transition $n = 2 \rightarrow 1$ of the Fe^{+21} ion is also shown in Figure 3. The differences are obvious.

The redshift effect (item 3 above) conveniently provides a mechanism in favor of the emergence of Cerenkov line emission, particularly from dense clouds. Obviously, for an opaque, optically thick dense gas, the emergent line flux from the surface of the cloud is determined by the competition between emission and absorption. The absorption mechanism for a Cerenkov line is drastically different from that for a normal line. A normal spectral line, exactly located at $\lambda = \lambda_{lu}$, would be greatly weakened by a strong resonant line absorption because the line absorption coefficient $k_{lu}(\lambda = \lambda_{lu})$ at $\lambda = \lambda_{lu}$ is very large (Fig. 2). In the case of a very dense gas, the emergent radiation simply becomes a blackbody continuum, and the normal line vanishes. In contrast, a Cerenkov line, which occurs at $\lambda > \lambda_{lu}$ as a result of the Cerenkov redshift, can avoid the strong line absorption because $k_{lu}(\lambda > \lambda_{lu}) \rightarrow 0$ (Fig. 2). Therefore, a Cerenkov line suffers only very small amounts of photoelectric absorption k_{bf} (the extremely weak free-free absorption k_{ff} in the X-ray band can be neglected), much smaller than the regular line absorption $k_{lu}(\lambda_{lu})$, i.e., $k_{bf} \ll k_{lu}(\lambda = \lambda_{lu})$. For example, for the iron Kα line, the dominant photoelectric absorption comes from the L-shell electrons of iron ions, for which the photoelectric absorption coefficient $k_{bf} \approx k_{bf}(\mathrm{Fe, L})$ is much smaller than the regular line absorption; that is, $k_{bf} \approx k_{bf}(\mathrm{Fe, L}) \ll k_{lu}(\lambda = \lambda_{lu})$. This means that the photons of the Cerenkov line can escape readily from deep inside a dense gas cloud; in other words, the dense gas would appear more "transparent" for the Cerenkov line emission than for a normal line produced by the spontaneous transition. It is probable that the optical depth of a dense cloudlet with size r can be less than one, $\tau = k_{bf}(\mathrm{Fe, L})r < 1$, despite the high density of iron ions N_{Fe}; i.e., the dense cloudlet possibly becomes optically thin for the peculiar Cerenkov line emission. Even in the optically thick case, $\tau = k_{bf}(\mathrm{Fe, L})r > 1$, the Cerenkov emission layer at the surface of the dense cloud with thickness $l \sim 1/k_{bf}(\mathrm{Fe, L})$ would still be surprisingly thicker than that for the normal line. An optically thin case or a thick Cerenkov emission layer at the surface of an opaque dense gas region means the possibility of very strong emergent Cerenkov line emission, as long as there are a sufficient number of relativistic electrons near the surface. It is possible that the Cerenkov line emission is even predominant over the markedly suppressed normal fluorescence line in such special cases.

3. MODEL CONSIDERATIONS AND CALCULATIONS

3.1. *Model Considerations: New Scenario*

As mentioned above, the Cerenkov line–like radiation may be particularly important in astrophysical environments with a very high gas concentration and with abundant relativistic electrons. One such example would be AGNs, particularly the Seyfert 1 galaxies, for which the

existence of dense gas regions seems plausible. The gas at the surface of an AGN disk is thought to be compressed to very high density by the high radiation pressure of the coronal X-rays. However, although the disk-type geometry is compatible with the Cerenkov mechanism, in the following model consideration we prefer to adopt the quasi-spherical distribution of dense cloudlets with spherical, filamentary-like, or sheetlike shapes around the central black hole, in order to avoid some defiances on the validity of disk models (Sulentic, Marziani, & Calvani 1998a; Sulentic et al. 1998b). The possible presence of such dense clouds, filaments, and sheets in AGN environments has been discussed by Rees (1987), Celotti, Fabian, & Rees (1992), Kuncic, Blackman, & Rees (1996), Kuncic, Celotti, & Rees (1997), and Malzac (2001). The clouds must be very dense to remain cool and therefore held by magnetic fields. Cool gas trapped by the magnetic field is compressed to extreme densities by the high radiation pressure, which is similar to what happens at the surface of the disk surrounding the central supermassive black hole. Recently some authors adopted the quasi-spherical distribution of dense cloudlets to explain the origin and profile of the iron Kα line (Karas et al. 2000; Collin-Souffrin et al. 1996; Brandt & Gallagher 2000). In their scenario, the innermost part of the disk is disrupted as a result of disk instabilities. Part of the disrupted material forms the optically thick, cold cloudlets of dense gas that cover a significant portion of the sky from the point of view of the central X-ray source, while the rest gets heated up to high temperatures, forming a corona (see Fig. 4). Recent observations support the existence of dense clouds or filaments in AGNs (Boller et al. 2002), which strongly favors the operation of the Cerenkov line–like radiation mechanism.

Figure 4 sketches the schematic of our working model of a quasi-spherical emission region around the central supermassive black hole of an AGN. In Figure 4 the shaded circles or strips represent cool cloudlets or filaments of dense gas. The dotted region stands for the hot, rarefied corona. The tiny dots, uniformly distributed in the corona, represent thermal electrons, and the bold dots represent the relativistic electrons, which are highly concentrated around the cloudlets in the corona (for reasons see below).

Evidence also seems to be mounting on the existence of abundant relativistic electrons. It is likely that the observed power-law continuum over a very wide frequency range, from radio to UV, is largely attributed to nonthermal radiation of relativistic electrons.[6] Although the detailed mechanism to produce an excessive amount of high-energy electrons remains unclear, flare events or some shock processes in the corona may be responsible. Such shock processes also take place in the gamma-ray burst events, in which ultrafast electrons are produced by the internal and external shock waves, thus producing the nonthermal radiation. The strong shock waves originate from drastic release of gravitational energy during the mergers processes, e.g., the neutron star–neutron star or the neutron star–black hole mergers (Piran 1999; Meszaros 2002). It is probable that similar processes also occur in AGN environments. The biggest difference between the accretions of the AGN supermassive black hole and the small black hole with solar mass could be that the accreted matter moving around the AGN black hole is not in a pure gas state. Many components could be coexistent and mixed in regions proximate to the central black hole. Except for the dense cloudlets, there exist

[6] However, there is no clear evidence for X-ray emission from highly relativistic electrons in Seyfert galaxies.

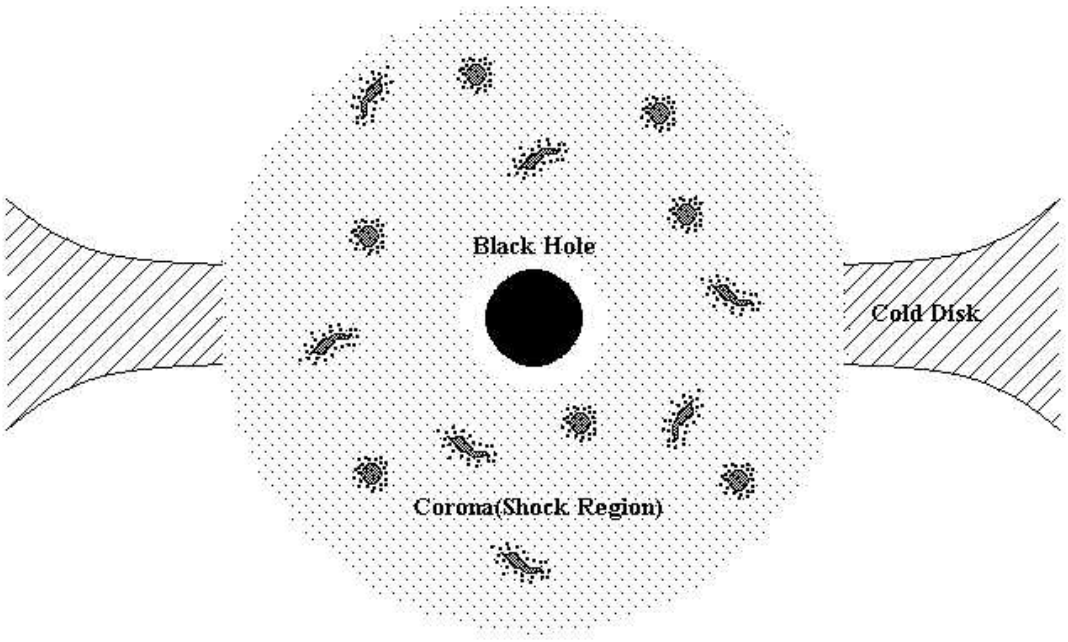

FIG. 4.—Schematic sketch of the emission region of the iron Kα line around a central supermassive black hole of AGNs. The shaded circles or strips represent cloudlets or filaments consisting of cold dense gas. The dotted region is the hot, rarefied corona where the tiny dots and the bold dots represent thermal electrons and relativistic electrons, respectively. The thermal electrons have a uniform distribution but the relativistic electrons have a high concentration around the clouds and/or filaments.

the solid debris and fragments, the meteorites and planets, and even the stars, e.g., the neutron stars and the black holes with star mass. The frequent collisions and mergers between these objects should be expected, e.g., the mergers of meteorite–neutron star and mergers of planet–black hole, which also produce a chain of "merger–drastic release of gravitational energy–strong shock–plenty of fast electrons," although the scale of energy release in each merger could be much smaller than that in gamma-ray bursts. Given the ubiquity of shock events in the corona region around the central supermassive black hole and their frequent collisions with dense clouds, the whole region of iron line emission is regarded as a shock-filled X-ray source (Fig. 4). The collisions convert part of the kinetic energy of the shock wave to thermal energy of the relativistic electrons (see, e.g., Piran 1999). Obviously, most fast electrons thus produced are concentrated in a narrow zone that closes to the collision front at the surface of the dense cloudlet (or on the flare spots if they are produced in flare events), as shown in Figure 4. Diffusion of fast electrons outward to ambient space is expected to be slow as a result of the trapping effect of magnetic fields near the clouds or flares. The ability to retain extremely high concentration of relativistic electrons near the dense clouds undoubtedly provides a very favorable environment for the operation of the Cerenkov line emission.

If the conditions, namely, the existence of dense gas and relativistic electrons, are met, the Cerenkov line–like emission becomes inevitable.

3.2. *Model Calculation*

Now we derive the intensity or luminosity of the Cerenkov line, in particular the iron Kα line, under various environmental parameters and compare it with observations. Except for the geometric size of the emission region, the main factors that determine the luminosity of the Cerenkov line include the density of the iron ions $N_{\rm Fe}$, the density of the relativistic electrons N_e, and the average or typical energy γ_c of the relativistic electrons, where the Lorentz factor $\gamma \equiv 1/(1-\beta^2)^{1/2} = mc^2/m_0c^2$ represents the dimensionless energy of an electron in units of m_0c^2. Our goal is to estimate the (range of) values of N_e, $N_{\rm Fe}$, and γ_c under a fixed size D of the emission region from the theory of Cerenkov line radiation (You et al. 2000), to match the observed luminosities of the iron Kα line and, in turn, to see whether these values are acceptable in the environment of AGNs.

In this paper our main interest is in the energetics of the iron Kα emission process; therefore, we leave out lengthy discussion on the line profile, except to note that even though a Cerenkov line is intrinsically broad, asymmetric, and redshifted, it is still insufficient to produce the highly skewed emission features observed in AGNs. A supermassive black hole is still needed to provide the necessary Doppler broadening and gravitational redshift.

We assume a typical mass $M \sim 10^7$–$10^8\ M_\odot$ for the central black hole. From the observed variation timescales of the iron Kα line ($\sim$1 lt-day; see Nandra et al. 1997a; Done, Madejski, & Zycki 2000), we infer the size of the emission region to be $D \sim 10^{15}$–10^{16} cm. In the following model calculations, we adopt a typical value $D \approx 3 \times 10^{15}$ cm, or about $\sim 10^2 R_{\rm Sch}$–$10^3 R_{\rm Sch}$, where $R_{\rm Sch}$ is the Schwarzschild radius. To simplify the calculation, we assume all of the dense gas regions in the form of spherical cloudlets with the same radius, except to note that in reality they will naturally be in various cloudlike, filament-like, or sheetlike shapes with various sizes. As noted before, because of the strong irradiation from the central X-ray source, there should exist a photoionized layer at the surface of a cloudlet. The main species of the iron ions in this layer should be in the intermediate-ionization states, e.g., those from Fe^{+18} to $\sim Fe^{+21}$, because in many cases the observed line centers are around $\sim$6.47–6.5 keV (e.g., Wang et al. 1998; Weaver et al. 2001). Denoting the total number of cloudlets in the whole emission region as $\tilde{N}$ and the radius of each cloudlet as r, the covering factor of cloudlets to the central X-ray source is thus

$$f_c = \frac{\tilde{N}\pi r^2}{4\pi D^2} = \frac{\tilde{N} r^2}{4D^2}\ , \tag{1}$$

which must be less than unity to ensure the central X-ray source to be only partly covered.

From equation (1) we see that the unknown quantity $\tilde{N}r^2$ can be removed by f_c and D. The volume filling factor is

$$f_v = \frac{\tilde{N} 4\pi r^3/3}{4\pi D^3/3} = \tilde{N}\frac{r^3}{D^3}\ . \tag{2}$$

Therefore, the ratio is $f_v/f_c \approx r/D$, which means that the fractional volume occupied by the cloudlets would be very small if $r \ll D$. At the same time, $\tilde{N}$ can be still very large to maintain a necessarily large covering factor f_c.

In order to avoid the ambiguity of our quantitative analysis, the following is restricted to calculate the Cerenkov line emission in the optically thick case, although the optically thin case is also possible in AGNs.

The emergent intensity of the Cerenkov iron Kα line from the surface of the optically thick dense gas is (eq. [A12] in the Appendix, or eq. [42] in You et al. 2000)

$$I^c_{\rm K\alpha} = Y\left[\ln\left(1+X^2\right) - 2\left(1 - \frac{\arctan X}{X}\right)\right] \quad \left(\text{ergs s}^{-1}\ \text{cm}^{-2}\ \text{sr}^{-1}\right)\ , \tag{3}$$

where the parameter $Y \equiv N_e C_1/2k_{\rm bf} \propto N_e$, the density of relativistic electrons, and $X \equiv (k_{\rm bf}/C_2)^{1/2} C_0 \gamma_c^2 \propto \gamma_c^2 N_{\rm Fe}$, where $N_{\rm Fe}$ and γ_c represent the density of iron ions in gas cloudlets and the typical (or average) energy of the relativistic electrons, respectively. C_0, C_1, C_2, and $k_{\rm bf} \approx k_{\rm bf}({\rm Fe, L})$, included in X and Y, are the parameters that are dependent on the density $N_{\rm Fe}$ and the atomic parameters of concerned ions, e.g., the frequency ν_{lu} (or $h\nu_{lu} \equiv \varepsilon_{lu}$) and the transition probability A_{ul} (eq. [A11] in the Appendix, or You et al. 2000). Inserting the concerned atomic parameters of the iron ions, for iron Kα line, $u = 2, l = 1$, we obtain

$$X \equiv \sqrt{\frac{k_{\rm bf}}{C_2}} C_0 \gamma_c^2 = 6.49 \times 10^{-28} g_2 \sqrt{\frac{S_2}{g_2}\left(\frac{S_1}{g_1} - \frac{S_2}{g_2}\right)} N_{{\rm Fe}\gamma_{c2}}\ ,$$
$$Y \equiv \frac{N_e C_1}{2k_{\rm bf}} = 0.16 \frac{g_2}{S_2}\left(\frac{S_1}{g_1} - \frac{S_2}{g_2}\right) N_e\ , \tag{4}$$

where g_2 and S_2 represent, respectively, the degeneracy and the real occupation number of electrons at the second level of the iron ion, so $S_2 \le g_2$. In addition, g_1 and S_1 are the corresponding quantities of the first level.

From equation (4) we see that in a physically reasonable environment in AGNs, it usually holds that $X < 1$.

Therefore, equation (3) is simplified as

$$I^c_{\mathrm{K}\alpha} \approx \frac{YX^2}{3} \ . \tag{5}$$

The Cerenkov line emission produced by the thermal relativistic electrons with random direction distribution of velocities is isotropic; thus, the Cerenkov intensity $I^c_{\mathrm{K}\alpha}$ is θ independent. Therefore, the emergent flux $F^c_{\mathrm{K}\alpha}$ from the surface of the dense cloud is simply obtained,

$$F^c_{\mathrm{K}\alpha} = 2\pi \int_0^{\pi/2} I^c_{\mathrm{K}\alpha} \cos\theta \sin\theta \, d\theta = \pi I^c_{\mathrm{K}\alpha} \quad \left(\mathrm{ergs\ s^{-1}\ cm^{-2}}\right) . \tag{6}$$

Hence, the elementary luminosity of the Cerenkov iron Kα line of each cloudlet is

$$l^c_{\mathrm{K}\alpha} = 4\pi r^2 F^c_{\mathrm{K}\alpha} = 4\pi^2 r^2 I^c_{\mathrm{K}\alpha} \quad \left(\mathrm{ergs\ s^{-1}}\right) . \tag{7}$$

Combining equations (1) and (7), the total luminosity of the Cerenkov iron Kα line from the whole emission region becomes

$$L^c_{\mathrm{K}\alpha} = \tilde{N} l^c_{\mathrm{K}\alpha} = 4\pi^2 r^2 \tilde{N} I^c_{\mathrm{K}\alpha} \approx 16\pi^2 D^2 f_c I^c_{\mathrm{K}\alpha} \quad \left(\mathrm{ergs\ s^{-1}}\right) . \tag{8}$$

Inserting equations (4) and (5) into equation (8), taking $D \approx 3 \times 10^{15}$ cm, $f_c \approx 0.1$, and $S_1 = g_1 = 2$, we obtain

$$L^c_{\mathrm{K}\alpha} = 2.08 \times 10^{-22} \left(1 - \frac{S_2}{g_2}\right)^2 N_e N^2_{\mathrm{Fe}} \gamma_c^4 \quad \left(\mathrm{ergs\ s^{-1}}\right). \tag{9}$$

Comparing the Cerenkov luminosity of iron Kα line equation (9) with the typical observed value for Seyfert 1 galaxies, i.e., $L^{\mathrm{obs}}_{\mathrm{K}\alpha} \approx 10^{40}$–$10^{41}$ ergs s^{-1}, and letting $L^c_{\mathrm{K}\alpha} \approx L^{\mathrm{obs}}_{\mathrm{K}\alpha}$, we obtain

$$N^2_{\mathrm{Fe}} \gamma_c^4 N_e \approx 4.8 \times 10^{61} \left(1 - \frac{S_2}{g_2}\right)^{-2} \approx 10^{62} , \tag{10}$$

where for iron ions in intermediate-ionization states we take $S_2 \approx 1$–5, which corresponds to iron ions Fe^{+19}–Fe^{+23}. Equation (10) gives the combination condition for the iron density N_{Fe}, the density of fast electrons N_e, and the average or typical energy γ_c of the fast electrons to produce the Cerenkov luminosity of the iron Kα line that can be compared with the observed value.

Table 1 lists several tentative sets of parameters under the condition where we arbitrarily fix $N_e = 10^{12}$ cm^{-3}. The choice of combinations is somewhat arbitrary because so far the environments in AGNs are still not well understood. Some of these parameters may at first appear defiant to the current paradigm around the AGN black holes. In the following section we give discussions on the reasonableness of these parameters and acceptability of the related new scenario around the supermassive black hole in AGNs.

TABLE 1

Combinations of Iron Density, Characteristic Energy, and Density of Relativistic Electrons for Calculation of Cerenkov Luminosity of Iron Kα Line

N_{Fe} (cm^{-3})	γ_c	N_e (cm^{-3})
10^{13}	10^6	10^{12}
10^{14}	3×10^5	10^{12}
10^{15}	10^5	10^{12}
10^{16}	3×10^4	10^{12}
10^{17}	10^4	10^{12}

4. CONCLUSIONS AND DISCUSSIONS

In this paper we tentatively propose another mechanism—the Cerenkov line–like radiation—to study the origin of the elusive iron Kα feature in AGNs. The charming advantage of this new emission mechanism is that the radiation energy of the Cerenkov line is provided by the relativistic electrons rather than by the X-ray continuum. Therefore, the continuum and the iron Kα line emission are two components independent of each other. Hence, the lack of correlation between the line and the continuum fluxes can be understood in this way. We further give some model calculations to show the effectiveness of the Cerenkov mechanism to explain the AGN observations. We show that the calculated Cerenkov iron Kα line is strong enough to compare with observations of AGNs, only if the iron density N_{Fe} in the dense gas, the density of fast electrons N_e, and the characteristic energy of fast electrons γ_c are high enough, as shown in Table 1.

If the iron Kα feature indeed arises from the Cerenkov line mechanism, Table 1 signifies the possibility of a strikingly different scenario around the supermassive black hole in AGNs, with much denser, more violent, and more energetic environments than conventionally believed. In the following we discuss the reasonableness and acceptability of the new scenario.

First, what are the consequences if there exist abundant relativistic electrons with exceedingly high energies? The problem is that, except for the Cerenkov line–like radiation, the fast electrons also contribute substantially to the continuum radiation in the high-energy band through the inverse Compton scattering process (the synchrotron mechanism becomes unimportant in a very dense gas). The Compton power of a fast electron with energy γ_c passing through an X-ray field with energy density U_{ph} is as high as $p^{\mathrm{Comp}} \approx 2.6 \times 10^{-14} U_{\mathrm{ph}} \gamma_c^2 \approx 10^{-15} \gamma_c^2$ ($U_{\mathrm{ph}} \approx 0.1$ ergs cm^{-3} for typical Seyfert 1 galaxies). If the density and the energy of the fast electrons are as high as $N_e \approx 10^{12}$ cm^{-3} and $\gamma_c \approx 10^4$–10^5, as shown in Table 1, the Compton luminosity of the continuum in the whole emission region with size $D \sim 10^{15}$ cm would be unacceptably higher than the typical observed value $L \approx 10^{44}$ ergs s^{-1}. Another related problem is that, if both the iron K line emission and a significant portion of the continuum radiation owing to the inverse Compton scattering process originated from the same group of fast electrons, again the correlation between the fluxes of iron K line and the X-ray continuum would be expected, as in the case of the fluorescence model.

We envisage a solution to overcome the difficulties mentioned above. As pointed out in § 3, the fractional volume occupied by the cloudlets, where most of the fast electrons reside, can be very small compared with the overall volume of the X-ray emission region $V = (4\pi/3)D^3$, i.e., $f_v \ll 1$. In this case, the total number of fast electrons may not be large; thus, the corresponding Compton luminosity of the continuum $L^{\mathrm{Comp}} \approx f_v[(4\pi/3)D^3] N_e p^{\mathrm{Comp}}$ would be several orders lower than the typical value of the observed continuum luminosity $L \approx 10^{43}$–10^{44} ergs s^{-1}. A small f_v with a large f_c is readily realized as long as $r \ll D$, as mentioned in § 3. For

example, taking $D \sim 10^{15}$ cm, $r \sim 10^6$–10^7 cm, and $f_c \sim 0.1$, the filling factor is as small as $f_v \sim 10^{-10}$ to 10^{-9}, and hence we get $L^{\rm Comp} \ll L^{\rm obs} \sim 10^{44}$ ergs s^{-1}.

Another potential problem concerns the very high density of gas. If $N_{\rm Fe}$ is as high as those shown in Table 1, even up to $\sim 10^{16}$–10^{17} cm^{-3}, and if a cosmological abundance in AGNs is assumed, then the inferred gas density would be inconceivably high. Therefore, an abnormally high iron abundance is necessary to restrict the total gas density at an acceptable level. We envisage two possibilities as follows: either frequent nuclear reactions in the vicinity of the central black hole or a phase transition to form dusty clouds in dense gas regions could be responsible for the marked increase of abundance of iron and other heavy elements without enhancement of gas density. In the latter case, the iron ions may be locked up in tiny grains as an embedded impurity. A high density of impurity iron is achievable in a heavily doped solid, even as high as $N_{\rm Fe} \sim 10^{16}$–10^{17} cm^{-3}. It is conceivable, in principle, that the Cerenkov line–like radiation of iron ions may also occur in the impurity-doped dust, as in the gas medium. Undoubtedly, the Cerenkov line–like radiation from the impurity-doped solid would be a challenging problem in future experimental physics. Existence of dusty clouds with iron-rich grains in the environments of AGNs would be equally mind boggling in black hole physics.

Finally, we consider the reasonableness of the energetics of our model. As we suggested in § 3, the relativistic electrons, necessary for the Cerenkov line–like radiation mechanism, are produced, for example, by the strong shocks, which originate from the merger processes. However, the energy that goes into the relativistic electron population in this way could only be a small fraction of the total. In this case, it would be important to give a more comprehensive physical consideration of the "efficiency of energy transformation from the kinetic energy of shock to the thermal energy of relativistic electrons." We hope to give a moderate solution in the future.

We are sincerely grateful to Christopher S. Reynolds at the University of Maryland for his helpful discussions and suggestions, which helped us to greatly improve this paper. The work of J. H. Y. is supported by the Natural Science Foundation of China, grant 19773005. W. P. C. acknowledges the grant NSC91-2112-M-008-043 from the National Science Council.

APPENDIX

BASIC FORMULAE FOR CERENKOV LINE–LIKE RADIATION

We first emphasize that the CGSE system of units was used in this appendix. This means, in particular, that all energies of X-ray photons in the following formulae will be in ergs rather than keV (1 keV $= 1.602 \times 10^{-9}$ ergs). Besides, one can find the detailed derivation of the following basic formulae in our published paper (You et al. 2000).

A1. THE REFRACTIVE INDEX n AND THE EXTINCTION COEFFICIENT κ

The essential point of the calculation of the spectrum of Cerenkov radiation is the evaluation of the refractive index of the gaseous medium. This is easy to understand qualitatively from the necessary condition for producing Cerenkov radiation, $v > c/n_\nu$. At a given frequency ν, the larger the index n_ν, the easier it is to satisfy the condition $v > c/n_\nu$, and the stronger the Cerenkov radiation at ν will be. Therefore, in order to get the theoretical spectrum of Cerenkov radiation, it is necessary to calculate the refractive index n_ν and its dependence on ν (the dispersion curve $n_\nu \sim \nu$). For a gaseous medium, the calculation is easy to do. Omitting the detailed derivation, here we only give the expressions of the index n_ν and the extinction coefficient κ_ν of gas as follows:

$$n_\nu^2 - 1 = \frac{C^3 h^4}{16\pi^3} \varepsilon_{lu}^{-4} A_{ul} g_u N_{\rm Fe} \left(\frac{S_l}{g_l} - \frac{S_u}{g_u} \right) y^{-1} ,$$
$$\kappa_\nu = \frac{C^3 h^4}{128\pi^4} \varepsilon_{lu}^{-5} \Gamma_{lu} A_{ul} g_u N_{\rm Fe} \left(\frac{S_l}{g_l} - \frac{S_u}{g_u} \right) y^{-2} \qquad \left(\text{when } y \geq 10^{-5}\right) , \tag{A1}$$

where $\varepsilon_{ul} \equiv h\nu_{ul} = \varepsilon_u - \varepsilon_l$ represents the energy of the line photon, ε_u and ε_l are the energies of the upper and lower levels of the iron ion, respectively (for definiteness in the following, we are only concerned with the Cerenkov iron line, particularly the iron Kα); A_{ul} is Einstein's spontaneous emission coefficient for $u \rightarrow l$; $\Gamma_{ul} = \Gamma_u + \Gamma_l = \sum_{i<u} A_{ui} + \sum_{j<l} A_{lj}$ is the quantum damping constant for the atomic (ionic) line with energy ε_{ul}, which is related to Einstein's spontaneous emission probabilities A_{ui} and A_{lj}; $N_{\rm Fe}$ is the number density of iron ions in gas; g_u (or g_l) and S_u (or S_l) are the degeneracy and the actual occupation number of electrons of the upper level u (or lower level l), respectively; and $y \equiv \Delta\lambda/\lambda_{ul} = -\Delta\nu/\nu_{ul} = -\Delta\varepsilon/\varepsilon_{ul} = (\varepsilon_{lu} - \varepsilon)/\varepsilon_{lu}$ represents the fractional displacement of the frequency or photon energy. Here $y \ll 1$ as a result of the fact that Cerenkov line–like radiation concentrates in a narrow band $\varepsilon \approx \varepsilon_{ul}$.

A2. THE CERENKOV SPECTRAL EMISSIVITY J_ν^c (or J_ε^c)

The Cerenkov spectral emissivity can be derived from the dispersion curve $n_\nu \sim \nu$ given above. It is known from the basic theory of Cerenkov radiation that the power emitted in a frequency interval $(\nu, \nu + d\nu)$ or $(\varepsilon, \varepsilon + d\varepsilon)$ by an electron moving with velocity $\beta = v/c$ is $P_\nu\, d\nu = (4\pi^2 e^2 \beta\nu/c)(1 - 1/n_\nu^2\beta^2) d\nu$. Let $N(\gamma)d\gamma$ be the number density of fast electrons in the energy interval $(\gamma, \gamma + d\gamma)$ [$\gamma \equiv 1/(1-\beta^2)^{1/2} = mc^2/m_0c^2$ is the Lorentz factor, representing the dimensionless energy of the electron]. For an isotropic velocity distribution of the relativistic electrons as in normal astrophysical conditions, the Cerenkov

radiation will also be isotropic. Then the Cerenkov spectral emissivity $J_\nu^c\,d\nu$, or equivalently $J_y^c\,dy = J_\nu^c\,d\nu$, can simply be obtained by the integral $J_\nu^c\,d\nu = (1/4\pi)\int_{\gamma_1}^{\gamma_2} N(\gamma)d\gamma\,P_\nu\,d\nu$; thus, we get

$$J_y^c\,dy = C_1 N_e\left(y^{-1} - y_{\rm lim}^{-1}\right)dy\ , \tag{A2}$$

where N_e is the density of fast electrons, $y \equiv -\Delta\varepsilon/\varepsilon_{ul}$ is the fractional displacement of energy ε relative to intrinsic line energy $\varepsilon_{ul} \equiv h\nu_{ul}$, and $y_{\rm lim} = C_0\gamma_c^2$ is the fractional Cerenkov line width. C_0 and C_1 are the coefficients that are dependent on the density of iron ions $N_{\rm Fe}$ and the atomic parameters of concerned species of iron ions, as shown below.

A3. THE ABSORPTION COEFFICIENT

For an optically thick dense gas for which the Cerenkov line mechanism is more efficient, the final emergent intensity I_ν^c is determined by the competition between the emission J_ν^c (or J_ε^c) and the absorption k_ν. Therefore, it is necessary to consider the absorption of the gas at $\nu \approx \nu_{lu}$. For the optical and X-ray bands, only two absorption mechanisms are important for the Cerenkov line. One is the line absorption k_{lu} in the vicinities of atomic lines, which is directly related to the extinction coefficient κ_ν given in equation (A1) by a simple relation, i.e., $k_{lu} = 4\pi\nu\kappa_\nu/c$. Another is the photoelectric absorption $k_{\rm bf}$. The free-free absorption in the X-ray band is negligibly small. Thus, the total absorption is

$$k_\nu = k_{lu} + k_{\rm bf} = C_2 y^{-2} + k_{\rm bf}\ , \tag{A3}$$

where the coefficient C_2 depends on $N_{\rm Fe}$ and other atomic parameters, as C_0 and C_1 do. As a result of the fact that the line absorption decreases with $\Delta\nu = \nu - \nu_{lu}$ rapidly as $k_{lu} \propto y^{-2}$, $k_{lu}(\nu < \nu_{lu}) \to 0$. Therefore, in the whole actually effective frequency band of Cerenkov line emission, the dominant absorption is $k_{\rm bf}$. Particularly, for the iron Kα line that we consider, the dominant photoelectric absorbers are the L-shell electrons of iron ions. In this case, equation (A3) becomes

$$k_\nu = k_{lu} + k_{\rm bf} \approx k_{\rm bf} \approx k_{\rm bf}({\rm Fe, L}) \tag{A4}$$

and

$$k_{\rm bf}({\rm Fe, L}) = N_{\rm Fe} S_2 \sigma_{\rm bf}(2)\ , \tag{A5}$$

where S_2 is the occupation number of electrons in L shell (thus $S_2 \le g_2 = 8$) and $\sigma_{\rm bf}(2)$ is the cross section of photoelectric absorption of an L-shell electron. For an iron atom or ion, the hydrogen-like formula for the cross section is a good approximation, particularly for the low-lying levels $n = 2, 3$, i.e.,

$$\sigma_{\rm bf}(\nu, n) = \frac{32\pi^2 e^6 R_\infty Z^4}{3\sqrt{3}h^3\nu^3 n^5} g_{\rm bf}(\nu, T)\ . \tag{A6}$$

Inserting into equation (A5), taking the effective charge number $Z^{\rm eff} = 24$ for the L-shell electrons at level $n = 2$, and letting Gaunt factor $g_{\rm bf} \approx 1$, we get

$$k_{\rm bf}({\rm Fe, L}) \approx 8.4 \times 10^{-46} N_{\rm Fe} S_2 \varepsilon_{lu}^{-3}\ . \tag{A7}$$

A4. THE EMERGENT CERENKOV SPECTRAL INTENSITY AND CERENKOV TOTAL LINE INTENSITY

For a uniform plane-parallel slab, the emergent Cerenkov spectral intensity I_ν^c from the surface of the slab can be derived by using the equation of radiative transfer

$$I_\nu^c = \frac{J_\nu^c}{k_\nu}\left(1 - e^{-k_\nu L}\right)\ , \tag{A8}$$

where J_ν^c and k_ν (or J_y^c and k_y) are given by equations (A2) and (A3), respectively.

For optically thin gas, $\tau_\nu = k_\nu L \ll 1$; therefore, the Cerenkov line intensity is

$$I_\nu^c \approx J_\nu^c L. \tag{A9}$$

However, for a very dense gas, the Cerenkov emission slab becomes optically thick, thus equation (A8) can be simplified as $I_\nu^c \approx J_\nu^c/k_\nu$, or equivalently

$$I_y^c = \frac{J_y^c}{k_{lu} + k_{\rm bf}} = \frac{N_e C_1\left(y^{-1} - y_{\rm lim}^{-1}\right)}{C_2 y^{-2} + k_{\rm bf}}\ , \tag{A10}$$

where $y_{\rm lim} = C_0\gamma_c^2$ is the fractional Cerenkov line width. All of the atomic parameter-dependent coefficients C_0, C_1, C_2, and $k_{\rm bf}$

for iron ions are given as follows:

$$C_0 = 1.05 \times 10^{-76} \varepsilon_{lu}^{-4} A_{ul} g_u N_{\rm Fe} \left(\frac{S_l}{g_l} - \frac{S_u}{g_u} \right) ,$$

$$C_1 = 5.77 \times 10^{-53} \varepsilon_{lu}^{-2} A_{ul} g_u N_{\rm Fe} \left(\frac{S_l}{g_l} - \frac{S_u}{g_u} \right) ,$$

$$C_2 = 1.75 \times 10^{-87} \varepsilon_{lu}^{-4} A_{ul} \Gamma_{lu} g_u N_{\rm Fe} \left(\frac{S_l}{g_l} - \frac{S_u}{g_u} \right) ,$$

$$k_{\rm bf}({\rm Fe, L}) = 8.4 \times 10^{-46} \varepsilon_{lu}^{-3} S_2 N_{\rm Fe} \qquad \text{(only for iron K lines)} . \tag{A11}$$

For the iron Kα line, $u = 2$, $l = 1$. We emphasize again that the photon energy ε_{lu} in equation (A11) is in units of ergs (the CGSE units) rather than keV (1 keV $= 1.602 \times 10^{-9}$ ergs). Equation (A10) gives a broad and asymmetric profile of the Cerenkov line with a small Cerenkov line redshift, as shown in Figure 3.

Inserting equation (A10) into the integral $I^c = \int_0^{y_{\rm lim}} I_y^c \, dy$, we obtain the total line intensity I^c in the optically thick case,

$$I^c = Y \left[\ln(1 + X^2) - 2 \left(1 - \frac{\arctan X}{X} \right) \right] \qquad (\text{ergs s}^{-1} \text{ cm}^{-2} \text{ sr}^{-1}) , \tag{A12}$$

where $Y \equiv (N_e/2)(C_1/k_{\rm bf}) \propto N_e$, N_e being the density of relativistic electrons. $X \equiv (k_{\rm bf}/C_2)^{1/2} C_0 \gamma_c^2 \propto \gamma_c^2 N_{\rm Fe}$, where $N_{\rm Fe}$ and γ_c represent the density of iron ions in gas and the typical energy of relativistic electrons, respectively. Therefore, the total Cerenkov line intensity I^c is determined by the parameters N_e, $N_{\rm Fe}$, and γ_c. Inserting the atomic parameters of iron ions into equation (A11) for the iron Kα line, we obtain

$$X = 6.49 \times 10^{-28} g_2 \sqrt{\frac{S_2}{g_2} \left(\frac{S_1}{g_1} - \frac{S_2}{g_2} \right)} N_{\rm Fe} \gamma_c^2 ,$$

$$Y = 0.16 \frac{g_2}{S_2} \left(\frac{S_1}{g_1} - \frac{S_2}{g_2} \right) N_e . \tag{A13}$$

From equation (A13) we see, in a physically reasonable environment of AGNs, that we usually have $X < 1$, or equivalently, $N_{\rm Fe} \gamma_c^2 < 10^{27}$. Therefore, for the optically thick and $X < 1$ case, equation (A12) is simplified as

$$I_{{\rm K}\alpha}^c \approx \tfrac{1}{3} Y X^2 . \tag{A14}$$

X and Y are given by equation (A13) for the iron Kα line. In another extreme case, $X > 1$, or equivalently $N_{\rm Fe} \gamma_c^2 > 10^{27}$, equation (A12) is simplified as

$$I_{{\rm K}\alpha}^c \approx 2 Y (\ln X - 1) \approx 2 Y \qquad \text{for } X > 1 \text{ case} . \tag{A15}$$

REFERENCES

Boller, Th., et al. 2002, MNRAS, 329, L1
Brandt, W. N., & Gallagher, S. C. 2000, NewA Rev., 44, 461
Celotti, A., Fabian, A. C., & Rees, M. J. 1992, MNRAS, 255, 419
Chiang, J., et al. 2000, ApJ, 528, 292
Collin-Souffrin, S., Czerny, B., Dumont, A. M., & Zycki, P. T. 1996, A&A, 314, 393
Done, C., Madejski, G. M., & Zycki, P. T. 2000, ApJ, 536, 213
Fabian, A. C., Rees, M. J., Stella, L., & White, N. E. 1989, MNRAS, 238, 729
Fabian, A. C., et al. 2002, MNRAS, 335, L1
Guilbert, P. W., & Rees, M. J. 1988, MNRAS, 233, 475
Karas, V., Czerny, B., Abrassart, A., & Abramowicz, M. A. 2000, MNRAS, 318, 547
Kuncic, Z., Blackman, E. G., & Rees, M. J. 1996, MNRAS, 283, 1322
Kuncic, Z., Celotti, A., & Rees, M. J. 1997, MNRAS, 284, 717
Lee, J., Fabian, A. C., Brandt, W. N., Reynolds, C. S., & Iwasawa, K. 1999, MNRAS, 310, 973
Lee, J., Fabian, A. C., Reynolds, C. S., Brandt, W. N., & Iwasawa, K. 2000, MNRAS, 318, 857
Malzac, J. 2001, MNRAS, 325, 1625
Meszaros, P. 2002, ARA&A, 40, 137
Miniutti, G., Fabian, A. C., Goyder, R., & Lasenby, A. N. 2003, MNRAS, 344, L22
Nandra, K., George, I. M., Mushotzky, R. F., Turner, T. J., & Yaqoob, T. 1997a, ApJ, 477, 602
Nandra, K., George, I. M., Mushotzky, R. F., Turner, T. J., & Yaqoob, T. 1997b, ApJ, 488, L91
Piran, T. 1999, Phys. Rep., 314, 575
Rees, M. J. 1987, MNRAS, 228, 47P
Reynolds, C. S. 2001, in ASP Conf. Ser. 224, Probing the Physics of Active Galactic Nuclei by Multiwavelength Monitoring, ed. B. M. Peterson, R. S. Polidan, & R. W. Pogge (San Francisco: ASP), 105
Sulentic, J. W., Marziani, P., & Calvani, M. 1998a, ApJ, 497, L65
Sulentic, J. W., Marziani, P., Zwitter, T., Calvani, M., & Dultzin-Hacyan, D. 1998b, ApJ, 501, 54
Tanaka, Y., et al. 1995, Nature, 375, 659
Vaughan, S., Fabian, A. C., & Nandra, K. 2003, MNRAS, 339, 1237
Wang, J. X., Wang, T. G., & Zhou, Y. Y. 2001, ApJ, 549, 891
Wang, J. X., Zhou, Y. Y., Xu, H. G., & Wang, T. G. 1999, ApJ, 516, L65
Wang, T. G., Otani, C., Cappi, M., Leighly, K. M., Brinkmann, W., & Matsuoka, M. 1998, MNRAS, 293, 397
Weaver, K. A., Gelbord, J., & Yaqoob, T. 2001, ApJ, 550, 261
Xu, K. Z., Yang, B. X., & Xi, F. Y. 1981, Phys. Lett., 86, 24
———. 1988, Phys. Rev. A, 33, 2912
———. 1989, Phys. Rev. A, 40, 5411
You, J. H., & Cheng, F. H. 1980, Acta Phys. Sinica, 29, 927
You, J. H., Cheng, F. H., Cheng, F. Z., & Kiang, T. 1986, Phys. Rev. A, 34, 3015
You, J. H., Xu, Y. D., Liu, D. B., Shi, J. R., & Jin, G. X. 2000, A&A, 362, 762